Coupling of HDPE/hydroxyapatite composites by silane-based methodologies

R. A. SOUSA[1,2,3*], R. L. REIS[1,2], A. M. CUNHA[1], M. J. BEVIS[3]
[1]*Department of Polymer Engineering, University of Minho, 4800-058 Guimarães, Portugal*
[2]*3B's Research Group – Biomaterials, Biodegradables and Biomimetics, University of Minho, Campus de Gualtar, 4710-057 Braga, Portugal*
[3]*Wolfson Centre for Materials Processing, Brunel University, Uxbridge, Middlesex, UB8 3PH, UK*
E-mail: rasousa@dep.uminho.pt

Several coupling treatments based on silane chemicals were investigated for the development of high density (HDPE)/hydroxyapatite (HA) composites. Two HA powders, sintered HA (HAs) and non sintered HA (HAns), were studied in combination with five silanes, namely *y*-methacryloxy propyltrimethoxy silane (MEMO), 3-(2-aminoethyl)aminopropyltrimethoxy silane (DAMO), vinyltrimethoxy silane (VTMO), 3-aminopropyltriethoxy silane (AMEO) and trimethoxypropyl silane (PTMO). The HA particles were treated by a dipping in method or by spraying with silane solutions. After drying, the treated powders were compounded with HDPE or HDPE with acrylic acid and/or organic peroxide and subsequently compression molded. The tensile test specimens obtained from the molded plates were tensile tested and their fracture surfaces were observed by scanning electron microscopy (SEM). For the sintered HA (HAs) composites, the most effective coupling treatments concerning stiffness are those based on MEMO and AMEO. The low influence of these coupling procedures on strength is believed to be associated to the low volume fraction and the relatively smooth surface of the used HA particles. For the non-sintered HA (HAns) composites, it was possible to improve significantly both the stiffness and the strength. Amino silanes demonstrated to be highly efficient concerning strength enhancement. The higher effectiveness of the coupling treatments for HAns filled composites is attributed to their higher particle surface area, smaller particle size distribution and expected higher chemical reactivity. For both cases, the improvement in mechanical performance after the coupling treatment is consistent with the enhancement in interfacial adhesion observed by SEM.

1. Introduction

Materials that can be found in nature are the consequence of millions of years of continuous biological evolution. The morphological complexity of these materials, which bone is a perfect example, poses enormous technical challenges for those who try to replicate their unique behavior. Unfortunately, bone, as many other tissues, may require temporary or permanent substitution in traumatic or disease situations. For such cases, synthetic bone-analog materials that reproduce, up to a certain extent, the whole range of bone properties are of great medical interest. With the advances of tissue engineering, the scientific and technological basis for the substitution of damaged or deteriorated tissues by fully functional and compatible living equivalents are being launched. This will gradually reduce, in the coming years, the search for new synthetic materials for pure tissue substitution. Until the proper development and clinical introduction of such technology and the lack of better alternatives, synthetic bone substitutes can play a major role as biocompatible materials to be used in prosthesis, fracture fixation devices or other bone replacement applications.

Historically, bone fixation and total joint replacement have been accomplished with the use of metals that exhibit a much higher stiffness as compared with the typical modulus of bone (between 7 and 25 GPa) [1–3]. Under loading conditions, the differences in stiffness between the bone and the metal originates a stress-shielding effect, making most of the load to be carried by the fixation device that promotes osteoporosis phenomena [4, 5] or compromises tissue healing. So, it is crucial to replicate the bone mechanical behavior in materials for bone replacement and fixation in order to

* Author to whom all correspondence should be addressed.

surmount the problems associated with the stress-shielding effect of traditional metallic materials. Polymer-based composites can exhibit high stiffness and a clear anisotropic and viscoelastic behavior, which are typical characteristics of bone. This possibility has driven the development of the high density polyethylene (HDPE)/hydroxyapatite (HA) composites, proposed to be used as bone tissue substitute materials more than two decades ago by Bonfield *et al*. [6]. The concept relies on the combination of a ductile semi-crystalline polymer that can develop an anisotropic character by means of orientation techniques [7–9] reinforced with a stiff bone-like ceramic that ensures both the mechanical reinforcement and the bioactive behavior of the composite [10, 11].

A parallel research approach has been followed by the authors [12–16] for enhancing the mechanical performance of HDPE/HA composites. In fact, previous investigations have focussed on the control of the structure development and anisotropic character of HDPE [12] and HDPE/HA composites [13, 14] by means of: (i) using a non-conventional molding route; (ii) assessing alternative reinforcing systems like carbon fibers [15] and (iii) developing bioactive bi-composite moldings by means of selective reinforcement of the HDPE matrix with both HA and carbon fibers [16]. The integration of the above methodologies is expected to drive the successful development of bioactive and bicompatible composite materials for use in the orthopaedic field. At this stage, the mechanical behavior is constrained by factors such as the mechanical performance of the matrix, the length and alignment of the fibers and the interfacial interactions between the phases in both fiber reinforced and HA filled HDPE composites. Concerning the HA reinforcement, the efficiency of the particles as reinforcement agents for HDPE is reduced, due to its inherent low aspect ratio and low degree of chemical interaction with the HDPE phase. The successful development of appropriate chemical coupling routes is believed to be one of the several complementary possibilities for obtaining high mechanical performance composite materials aimed intended for use in high load bearing applications.

Silanes are recognized as adequate coupling agents for a variety of polymer composites [17–22]. Several works [23–26] claimed that silanes do interact with HA particles as well with bioactive glass [27], which confirms their potential to be used within the biomedical field. Nevertheless, their application in composites for biomedical applications is not straightforward, since these additives, when not covalently bonded, have the potential of leach out from the implant to the organism, which can cause toxic reactions to the surrounding tissues and compromise the biocompatibility of the bulk compound material. A previous study [28] on the biocompatibility of silane treated HA powders demonstrated acute toxicity of free silanes, but a biocompatible behavior for strongly adsorbed silanes on the HA surface. Furthermore, the *in vivo* studies by Shinzato *et al*. [27] indicated a decreasing trend of bone formation for increasing silane content in poly(methyl methacrylate)/bioactive glass composites. These works emphasized the importance of assuring a thin and chemically adsorbed silane layer on the HA surface that assures both the chemical coupling and the biocompatibility of the composite, but also avoids the existence of eventual leachable species.

Two studies by Liu *et al*. [29, 30] demonstrated reactivity of HA by means of hydroxyl groups at the particle surface. These groups can enable the covalent bonding of chemical species that are more prone to interact with functionalities of the long polymeric chains. In this perspective, the functionalization of the polyethylene is a complementary route for enhancing interaction between the polymer and the ceramic phases in HDPE/HA composites.

The aim of this study is to perform an exploratory investigation of several potential coupling methodologies to be used on HDPE/HA composites, based on two different modes of silane application to the HA powders for five different silanes. The treated powders were compounded with HDPE or HDPE with acrylic acid and/or organic peroxide and subsequently compression molded. The impact of the several coupling methodologies were evaluated by accessing their impact, on a comparative basis, on the mechanical performance and the interfacial adhesion.

2. Materials and methods

2.1. Materials

The high density polyethylene (HDPE) studied was a Hostalen GM 9255 F, supplied by Elenac GmbH (Kehl, Germany) with melt flow rates (MFR) of 0.37 ml/600 s (190 °C, 5 kg) and 12.0 ml/600 s (190 °C, 21.6 kg).

Two synthetic grades of hydroxyapatite (HA), supplied by Plasma Biotal Ltd (United Kingdom), were investigated: (i) a sintered HA and (ii) a non-sintered HA, further referred as HAs and HAns, respectively. These HA powders differ in terms of the granulometric dispersion and the specific surface area. The granulometric distribution of HAs powder exhibits sample and secondary modes at 12.9 and 5.3 μm, respectively; and an average particle size of 10.1 μm. HAns powder presents an unimodal granulometric distribution with a sample mode at 4.6 μm and an average particle size of 5.9 μm. The surface area of the hydroxyapatite powders are $0.38\,m^2/g$ ($1.19\,m^2/cm^3$) and $0.56\,m^2/g$ ($1.73\,m^2/cm^3$) for the sintered and the non sintered grades respectively.

Figs. 1 and 2 present a general and a detailed views of the HAs and the HAns particles respectively, as observed by scanning electron microscopy (SEM), together with the respective granulometric distribution curves. The HAs particles tend to form discrete agglomerates (Fig. 1(a)) and exhibit a relatively smooth surface (Fig. 1(b)). The agglomeration of the HAns particles is also evident (Fig. 2(a)) as well as their much smaller average particle size (Fig. 2(b)). The HAns powders exhibit a needle-like morphology.

Several silanes, from Dow Corning (USA), were used without further purification as coupling agents. The respective chemical formulas and designations are presented in Table I.

A powder form organic peroxide (2,5-bis(tert-butylperoxy)-2,5-dimethylhexane), incorporating silica as a

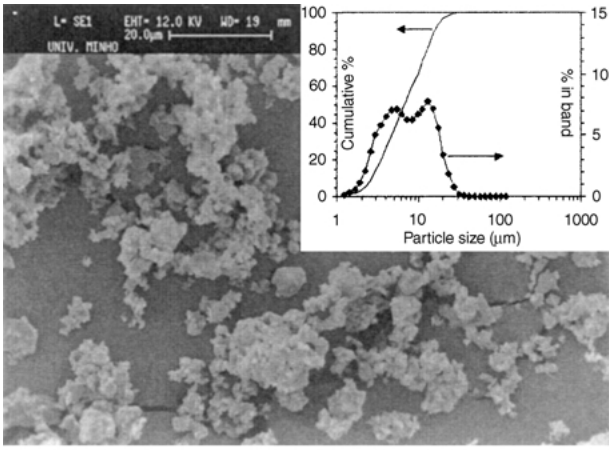

(a)

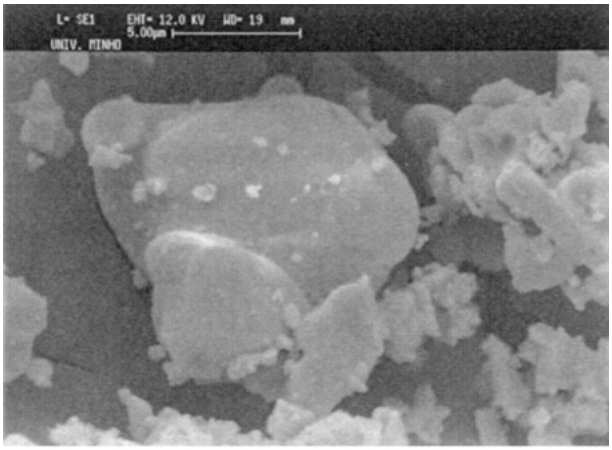

(b)

Figure 1 Scanning electron microscope (SEM) photographs of the HAs particles and respective granulometric distribution (a); and detailed view of the HAs particles (b).

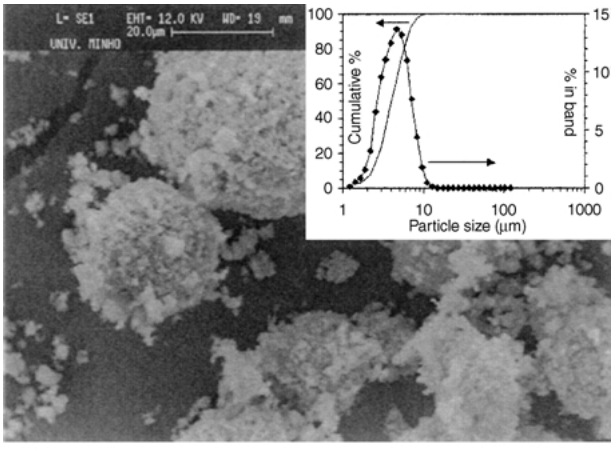

(a)

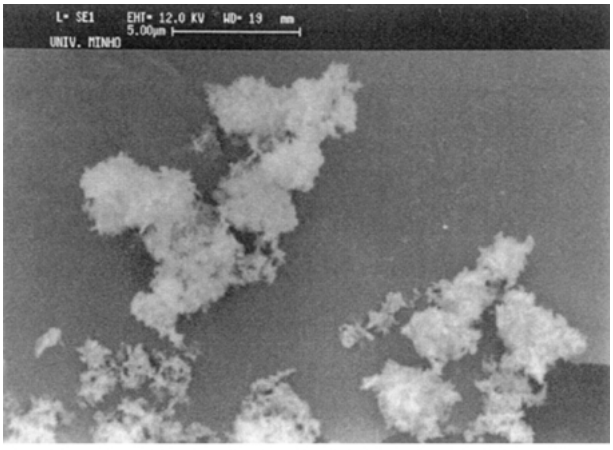

(b)

Figure 2 Scanning electron microscope (SEM) photographs of the HAns particles and respective granulometric distribution (a); and detailed view of the HAns particles (b).

carrier, Trigonox 101-45B, from Akzo Nobel (Sweden) was used in this study. This peroxide was chosen because of its relative slow decomposition rate at higher temperatures, which, in principle, allows sufficient time for mixing without premature decomposition during extrusion. An acrylic acid without further purification, from Aldrich (Germany) was also employed.

2.2. HA surface treatment methodologies

2.2.1. Spraying (SP)

In this case, the HA powders were spread over a surface and sprayed with a water/methanol (W/M) solution containing a silane amount corresponding to 1% by weight of the filler amount treated. Two types of solution were used: (i) neutral pH (pH of ~ 7.0), used for MEMO, DAMO, VTMO, PTMO and AMEO silanes (please see Table I for abbreviations); and (ii) pre-acidified with acetic acid (pH of ~ 4.5), used for MEMO, VTMO and PTMO silanes. Silane hydrolysis and stable silanol formation are enhanced for acidic pH ranges [32]. Following the spraying, the HA powders were dried in an oven under controled conditions of temperature and pressure [31].

2.2.2. Dipping in solution (SL)

The solutions were prepared by adding the silanes to distilled water or to mixtures of distilled water with methanol. The amount of silane by weight (S) in the solution varied between 0.21 and 1.00% relative to the

TABLE I Coupling agents studied and the respective abbreviations used in this study

Coupling agent	Abbreviation
y-methacryloxy propyltrimethoxy silane $CH_2=C(CH_3)–COO–(CH_2)_3–Si(OCH_3)_3$	MEMO
3-(2-aminoethyl)aminopropyltrimethoxy silane $H_2N–(CH_2)_2–NH–(CH_2)_3–Si(OCH_3)_3$	DAMO
vinyltrimethoxy silane $CH_2=CH–Si(OCH_3)_3$	VTMO
3-aminopropyltriethoxy silane $H_2N–(CH_2)_3–Si(OC_2H_5)_3$	AMEO
trimethoxypropyl silane $CH_3–C_2H_4–Si(OCH_3)_3$	PTMO

filler amount. Before the addition of the silane, the solutions were acidified to a range of pH between 4.5 and 5.0 with acetic acid (except for DAMO). The HA powders were subsequently dipped in the solution and stirred for a fixed amount of time. During this period, a chemical linkage is expected to occur through the reaction between the silanol and the hydroxyl groups available at the HA surface. This type of treatment was applied exclusively to HAns powders. After stirring, the slurries obtained were also dried in an oven under controlled conditions of temperature and pressure [31]. Both HA surface methodologies are schematically presented in Fig. 3.

2.3. Extrusion compounding and HDPE modification

The HA powders obtained according to the treatments described in Sections 2.2.1 and 2.2.2 were compounded with HDPE (10% wt HA) in combination, in specific cases, with 0.25% by weight (wt) organic peroxide (for VTMO only) or 0.25% wt organic peroxide plus 2.5% wt acrylic acid. Fig. 4 presents the schematic diagram of the extrusion compounding and the HDPE modification methods used for HDPE/HA composites. All the composites were compounded in a Leistritz AG-LSM 36/25D modular co-rotating twin screw extruder (TSE). The screw speed was 100 rpm and the temperature profile in the barrel (from feed to die zones) was 160/165/170/175/180/185/190/180 °C. The average output rate varied between 2.90 kg/h and 5.00 kg/h. The cooling of the extrudate was performed in air at an average temperature of 17 °C.

The low amount of HA used in this study for the composite materials (both HAs and HAns formulations) corresponds to a deliberate option in extending (without increasing costs too greatly), as much as possible, the number of coupling methodologies investigated in order to screen a large number of potential routes for interfacial interaction improvement. The composites incorporating the treated HA powders will be designated according to the respective treatment employed. The abbreviations employed for the HAs and the HAns based composites are presented respectively in Tables II and III for each treatment stage. The abbreviations include the type of silane, the sort of treatment (dipping in solution or spraying), the solvent nature (water, W; methanol, M; or mixture of these two, W/M), the acidity of the solution (pH refers to an acid pH solution by means of acetic acid

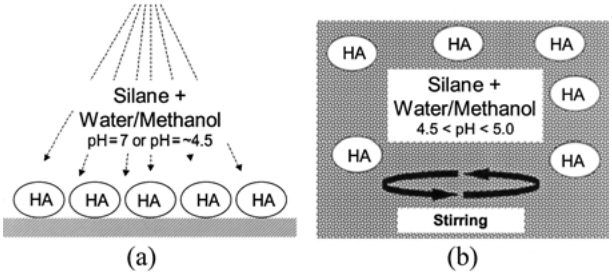

Figure 3 Schematic diagram of the HA surface treatment methodologies: (a) spraying; (b) dipping in solution.

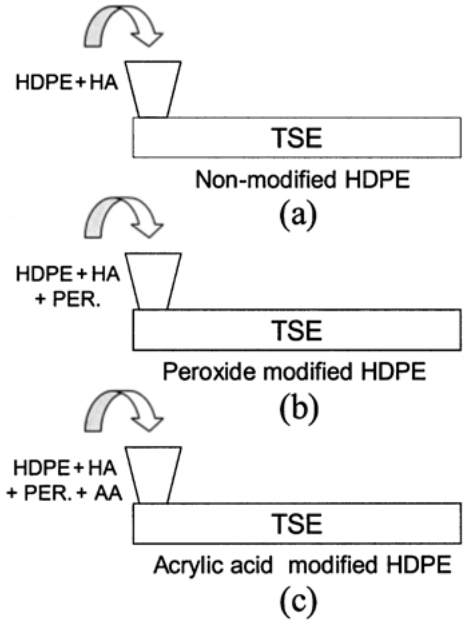

Figure 4 Schematic diagram of the extrusion compounding and HDPE modification methods used: (a) non-modified HDPE; (b) peroxide modified HDPE and (c) acrylic acid modified HDPE.

addition), the isolated use of peroxide (PER) or the use of both peroxide and acrylic acid (AA). As an example, HDPE/HAs VTMO pH PER refers to the composites of HDPE filled with sintered HA treated by spraying (SP) of a water/methanol solution of vinyltrimethoxysilane (VTMO) acidified with acetic acid; while HDPE/HAns MEMO refers to the composites of HDPE with non sintered HA powders treated by immersion in a water solvent solution (SL) of *y*-methacryloxy propyltrimethoxy silane (MEMO), with no acetic acid addition and no peroxide or acrylic acid. In case of doubt concerning designations employed for the various formulations here investigated, the reader is kindly asked to review Tables II and III.

2.4. Compression molding and tensile test samples preparation

The composite materials were molded by compression molding into rectangular plates with the dimensions of $2 \times 110 \times 160\,mm^3$. The compression molding was performed at 190 °C in two stages: (i) 5 min compression at 2.8 MPa and (ii) 7 min compression at 7.0 MPa. After compression, the cooling of the plates was achieved by quenching in water. Small dumb-bell tensile test specimens with rectangular cross section ($2 \times 4\,mm^2$) and 20 mm gauge length were cut from the molded plates using a proper die.

2.5. Tensile testing

The samples obtained were tensile tested on an Instron 4505 universal testing machine, using an Instron 2630 resistive extensometer with 10 mm of gauge length. These tests were performed in a controlled environment (23 °C and 55% RH) and aimed to determine the tangent modulus (E_t), the ultimate tensile strength (UTS) and the strain at break (ε_b). The cross-head speed was 5 mm/min

TABLE II Abbreviations for the HDPE/HAs based composites

Silane	HA surface treatment			HDPE modification		Designation
	Application mode SL, SP	Solvent W, M	Acetic acid pH	Peroxide PER	Peroxide + acrylic acid AA	
MEMO	SP	W/M				MEMO
					AA	MEMO AA
			pH			MEMO pH
					AA	MEMO pH AA
DAMO	SP	W/M				DAMO
					AA	DAMO AA
VTMO	SP	W/M		PER		VTMO PER
			pH			VTMO pH PER
AMEO	SP	W/M	pH			AMEO
					AA	AMEO AA
PTMO	SP	WM	pH			PTMO
					AA	PTMO AA

TABLE III Abbreviations for the HDPE/HAns based composites

Silane	HA surface treatment			HDPE modification		Designation
	Application mode SL, SP	Solvent W, M	Acetic acid pH	Peroxide PER	Peroxide + acrylic acid AA	
MEMO	SL	W	pH			MEMO SL
					AA	MEMO SL AA
	SP	W/M				MEMO SP
					AA	MEMO SP AA
			pH			MEMO SP pH
					AA	MEMO SP pH AA
DAMO	SL	W				DAMO SL W
					AA	DAMO SL W AA
		W/M				DAMO SL W/M
					AA	DAMO SL W/M AA
	SP	W/M				DAMO SP
					AA	DAMO SP AA
VTMO	SL	W	pH			VTMO SL W
				PER		VTMO SL W PER
		W/M				VTMO SL W/M
				PER		VTMO SL W/M PER
	SP	W/M				VTMO SP W/M
			pH			VTMO SP W/M pH
AMEO	SP	W/M	pH			AMEO
					AA	AMEO AA
PTMO	SP	W/M	pH			PTMO
					AA	PTMO AA

(8.3×10^{-5} m/s) until 1.5% strain, to determine more accurately the modulus, and then increased to 50 mm/min (8.3×10^{-4} m/s).

Following tensile experiments, *t*-student tests were applied in order to estimate the significance in mechanical performance results between the several coupling methodologies investigated. The discussion of the same is based on a confidence level of 99%, except when stated otherwise.

2.6. Scanning electron microscopy

Scanning electron microscopy (SEM) analysis was performed for fractographic analysis. Microscopy was performed on selected sets on a Leica Cambridge scanning electron microscope. All the surfaces were mounted on a copper stub and coated with Au/Pd alloy prior to examination.

3. Results and discussion

3.1. Mechanical performance

3.1.1. HDPE/HAs composites

Compression molded HDPE exhibits 1300 MPa of E_t. Upon 10% wt. HAs filling, the stiffness of HDPE is maintained (statistical support for eventual variation requires a confidence level below 79%). This result shows that the very low filler amount employed (10% by weight, approximately 4% by volume) is insufficient to enhance the rigidity of the matrix. The HDPE/HAs composites exhibit a ductile fracture, failing at the gauge length region during the work hardening of the sample. The tensile test results for the HDPE/HAs composites, in

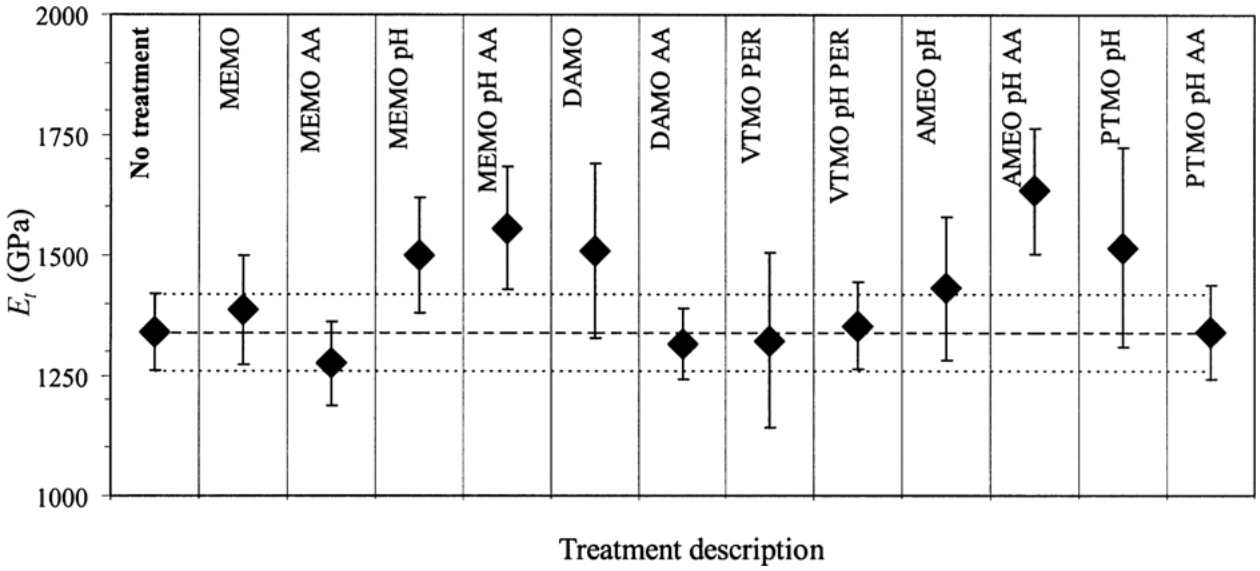

Figure 5 Tangent modulus (E_t) for the HDPE/HAs composites (10% wt).

terms of tangent modulus (E_t) are presented in Fig. 5. In spite of the low amount of HA employed, the coupling methodologies applied cause, in some cases, significant variations in stiffness when compared to the uncoupled HDPE/HAs composite.

Interpretation of mechanical performance variation of polymer matrices upon particulate filling should consider the influence of the filler on the crystallization kinetics of the matrix. Mineral particles can act as nucleating agents of the polymeric matrices [33, 34], which may affect the semicrystalline structure of the polymer matrix and consequently the mechanical behavior of the composite. This factor may be particularly relevant for low filler amounts, where the stiffening effect of the particles may be overlapped by the consequences of matrix crystallinity modification. Talc is an example of a nucleating agent in both polyethylene and polypropylene matrices [19, 35], where the use of silane coupling agents have a strong side effect on the definition of the talc activity as nucleating agent [19, 35]. For the present case, the variation in mechanical behavior for the coupled composites may eventually be justified not only by variations in the level of interfacial interaction, but also by dissimilarities in the semicrystalline structure of HDPE as induced by the presence of the treated particles. Although these considerations are important, the investigation of both the nucleating effect of HA particles and the effect of silanes on such role, if any, is not discussed in this study.

For the coupling methodologies based on MEMO, improvements in stiffness of 15 and 20% are achieved respectively for the MEMO pH and MEMO pH AA formulations. In contrast, the HDPE composites incorporating HAs powders treated in neutral media (MEMO and MEMO AA) do not exhibit any significant difference in terms of stiffness. The difference in mechanical performance, observed between the MEMO formulations with and without the HA treated in acidic pH, results from the different hydrolysis degree of the silane for the two pH media, being higher for the pH formulations which determines the effectiveness of the silane and consequently the improved mechanical performance exhibited. Increments in stiffness are also observed for the DAMO, AMEO pH, AMEO pH AA and PTMO pH composites. For the coupling methodologies based on AMEO, a 10% improvement in stiffness (as compared to uncoupled HDPE/HAs) is achieved for the AMEO pH formulation (statistically significant at 90% confidence level), which is further extended to 25% upon acrylic acid grafting for the AMEO pH AA formulation (statistically significant above 99% confidence level). These results show the dependence of the coupling procedures on treatment factors such as the organo-functional chemistry, the pH of the treatment solution and the adoption or not of acrylic acid grafting.

Concerning strength, the filling of the HDPE with HAs particles reduces significantly its ultimate tensile strength (UTS). HDPE exhibits 35.8 MPa of UTS, decreasing about 17% to 28.8 MPa upon HAs filling. The decrease in tensile strength can be explained by two factors: the HA particle shape and the degree of HDPE-HA interaction. HA particles present a low aspect ratio, which disfavors stress transfer during loading of the composite. Furthermore, interfacial interaction between the polymer and the ceramic phases is restricted to the mechanical interlocking of the HA particles by the matrix developed upon the shrinkage of the polymer during cooling. As a consequence of these factors, the effective load-bearing cross-section decreases upon HA filling, which justifies the observed decrease in tensile strength. Fig. 6 presents the tensile test results, in terms of UTS, for the HDPE/HAs composites, where none of the coupling procedures cause significant improvement in the tensile strength relatively to the uncoupled composite. In spite of this, significant improvements in tensile strength are observed within specific coupling formulations. This is the case of VTMO PER that exhibits 25.8 MPa of UTS, increasing to 29.2 MPa for the VTMO pH PER composition, which is attributed to the extended

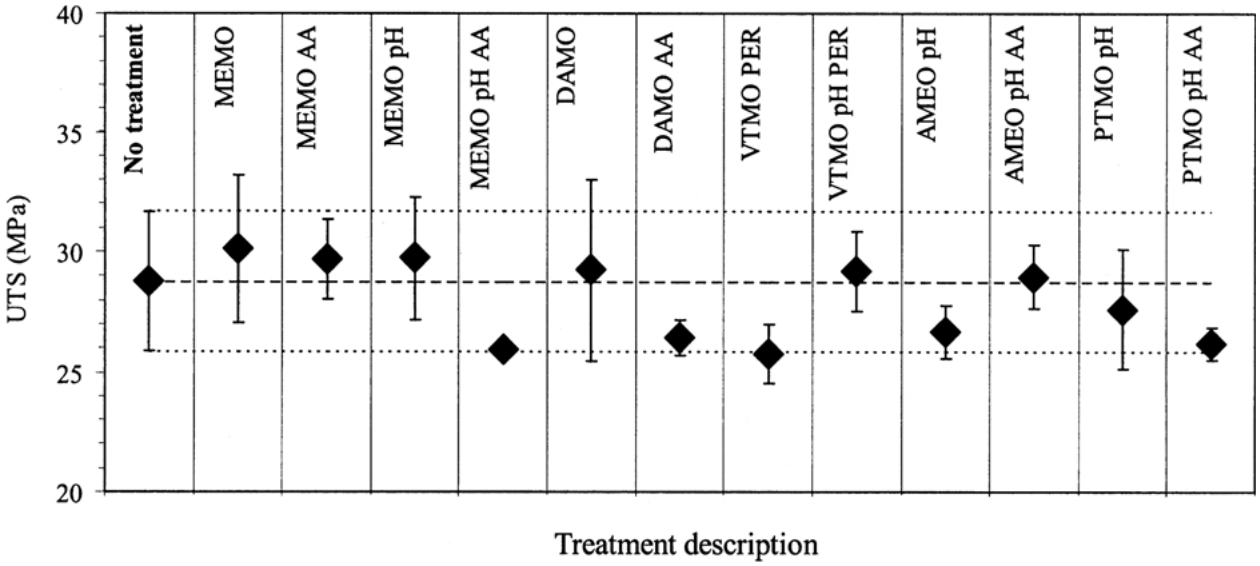

Figure 6 Ultimate tensile strength (UTS) for the HDPE/HAs composites (10% wt).

hydrolysis of the silane for the latter case. For AMEO, the grafting of acrylic acid produces an improvement in tensile strength (statistically significant at 90% confidence level). A previous investigation on the use of organotitanates and zirconates to HDPE/HA composites has shown that simultaneous improvement in stiffness and strength is achievable only by means of a filler dispersion improvement effect [14]. In the present study, the increase in strength from AMEO to AMEO AA are attributed to enhanced interfacial adhesion as result from acid/base interactions between the aminopropyl organofunctional groups of AMEO and the acrylic acid grafts. Such type of interaction has already been claimed to be responsible for enhanced interfacial interaction and improved tensile strength in low density polyethylene/glass fiber composites [21]. In some cases, the physical property improvement associated with silane coupling is not necessarily coupled with strength enhancement [19, 20]. In fact, a study by Velasco *et al.* [35] on HDPE/talc composites alleged silane to improve their stiffness without affecting their strength, while on HDPE/oil palm fibers composites, amino silanes showed a positive effect on the stiffness and no effect on strength, which was attributed to a dominant effect of factors such as filler agglomeration and filer shape on the composite mechanical performance [20]. For HDPE/HAs composites, the isolated improvements in stiffness observed herein are attributed to enhanced interfacial adhesion. However, the total interfacial area in the composite, defined by both the volume fraction and the surface area of the HA particles, is insufficient to achieve significant improvements in strength. It is believed that the low volume fraction and the relatively smooth particle surface restrain the effectiveness of the coupling treatment since the total modified interfacial area is too low to significantly alter the mechanical behavior of the composite at high strains.

Fig. 7 presents the variation of the strain at break (ε_b) for HDPE/HAs composites. HDPE presents 482% of ε_b. Upon HA filling, the ductility of HDPE is not affected for

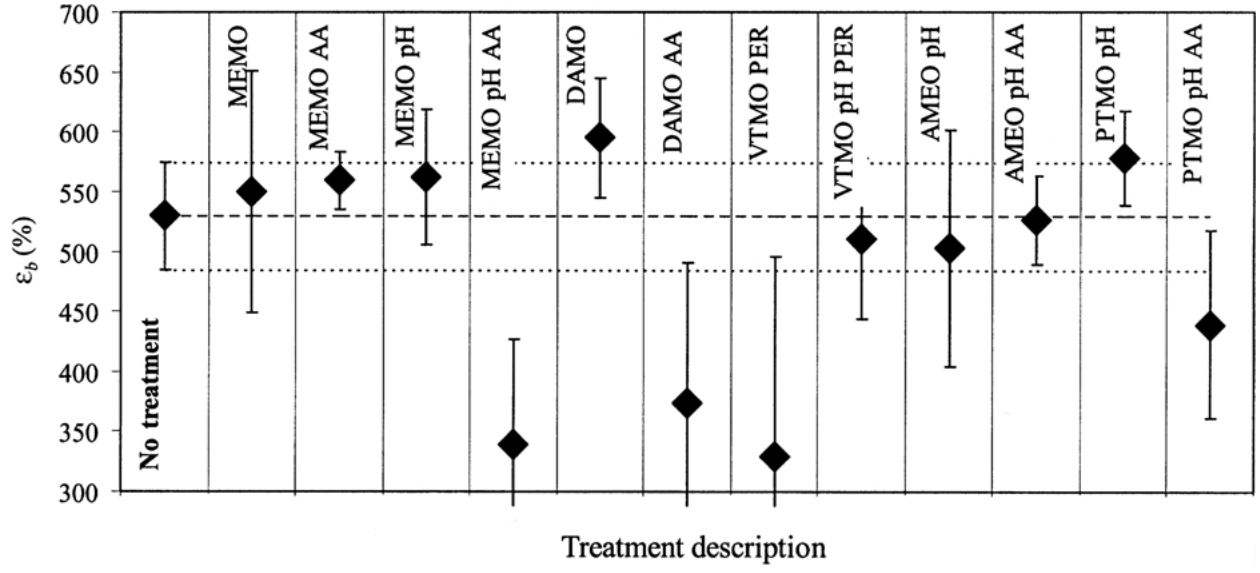

Figure 7 Strain at break (ε_b) for the HDPE/HAs composites (10% wt).

most of the coupling formulations, varying in a typical range of 500%. Exceptions occur for MEMO pH AA, DAMO AA and VTMO pH PER, with values of ε_b of respectively 340%, 373% and 330%. For all cases, it is evident the high standard deviations intervals associated to ε_b. The dispersion in ductility resulted from the inhomogeneous plastic deformation process observed during tensile testing for high values of strain. Apparently, compression molding does not introduce sufficient mixing in the composite to eliminate intergranular weldlines, making it more prone to premature failure at these points.

3.1.2. HDPE/HAns composites

HDPE/HAns present 1362 MPa of E_t, which does not statistically differ from that obtained for unfilled HDPE (differs for a confidence level below 67%). As previously observed for the HAs composites, the filling of HDPE with HAns particles does not alter the exhibited stiffness or the ductile mode of fracture. Nevertheless, the coupling methodologies investigated produce significant variations in stiffness as shown in Fig. 8 that presents the respective E_t for the various HDPE/HAns composites produced. The HA powders employed were treated and compounded according to the methods described in 2.2.1 and 2.2.2, respectively. For the coupling methodologies based on MEMO, MEMO SL exhibits 1559 MPa, which accounts for an increase of 14% as compared to the standard HDPE/HAns composite. Concerning the spraying treatments (SP), both the MEMO SP pH and the MEMO SP pH AA formulations exhibit higher stiffness values (significant at 95% confidence level) than the respective formulations incorporating HA treated in neutral pH solutions (MEMO SP and the MEMO SP AA, respectively), which shows once again the importance of the pH solution during silane hydrolysis. MEMO SP pH and MEMO SP pH AA present 1584 and 1541 MPa of E_t, which corresponds to increases in stiffness of 16 and 13%, respectively as compared to standard HDPE/HAns composites. This silane has been claimed to increase the interfacial adhesion between glass fibers and low density polyethylene, which was attributed to a reduction in the fibers polar character [22]. For the DAMO based coupling methods, the highest improvement in stiffness is obtained for DAMO SL W with a E_t of 1515 MPa, which indicates a suitability of amino silanes for improving the stiffness of HDPE/HA composites. From all the coupling methodologies investigated, the VTMO SL W/M composites exhibits one of the highest stiffness values with a E_t of 1625 MPa, which accounts for an increase of 20% as compared to the uncoupled composite. Upon peroxide addition in VTMO SL W/M PER, the stiffness decreases to 1409 MPa. The use of peroxide in VTMO SL W/M PER is intended to create free radicals, by displacing hydrogen from the HDPE chains, and promote covalent bonding with available vinyl organofunctional groups at the HA surface. A similar coupling strategy was highly successful in enhancing the stiffness and the strength of polypropylene/glass fiber composites [36]. The decrease in stiffness observed is probably related to a dominant effect of the peroxide initiated crosslinking of the matrix. A decrease in the polymer crystallinity occurs upon silane grafting [37] and polyethylene crosslinking [37, 38] that can sustain the respective decline in stiffness [39]. As for the HDPE/HAs composites, the AMEO based coupling methodologies (AMEO and AMEO AA) are effective in enhancing the stiffness of the composites (both statistically significant at 95% confidence level). The highest improvement is obtained for AMEO with a E_t value of 1571 MPa that corresponds to an increase of 13% as compared to standard HDPE/HAns composites.

As previously observed for HDPE/HAns composites, the HAns filling of HDPE decreases the composites tensile strength. However, some of the coupling methodologies are able to improve it significantly. Fig. 9 presents the tensile test results, in terms of UTS, for the HDPE/HAns composites. The superior efficiency of the coupling procedures for this filler is a direct consequence

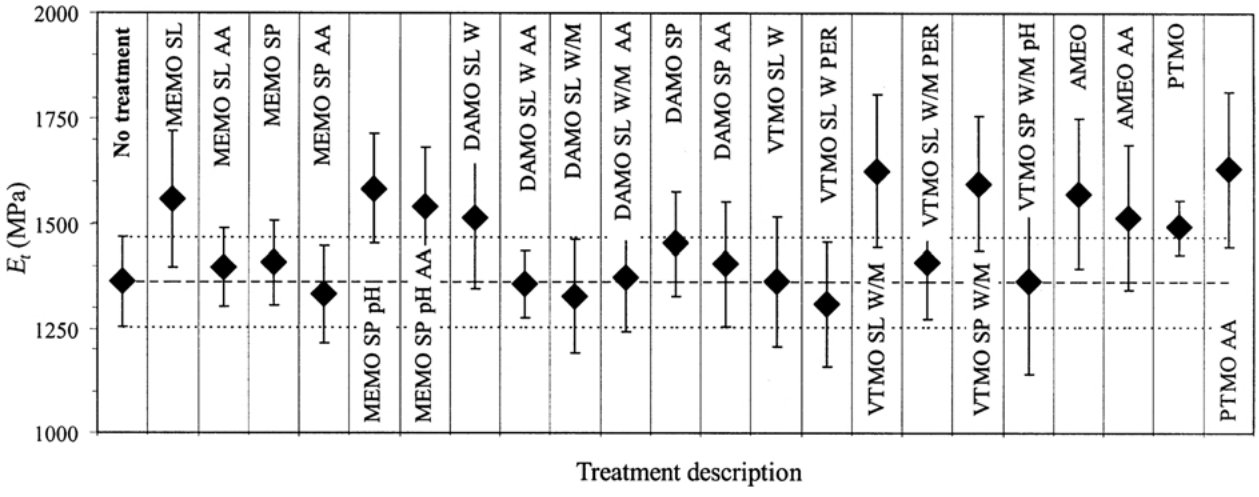

Figure 8 Tangent modulus (E_t) for the HDPE/HAns composites (10% wt).

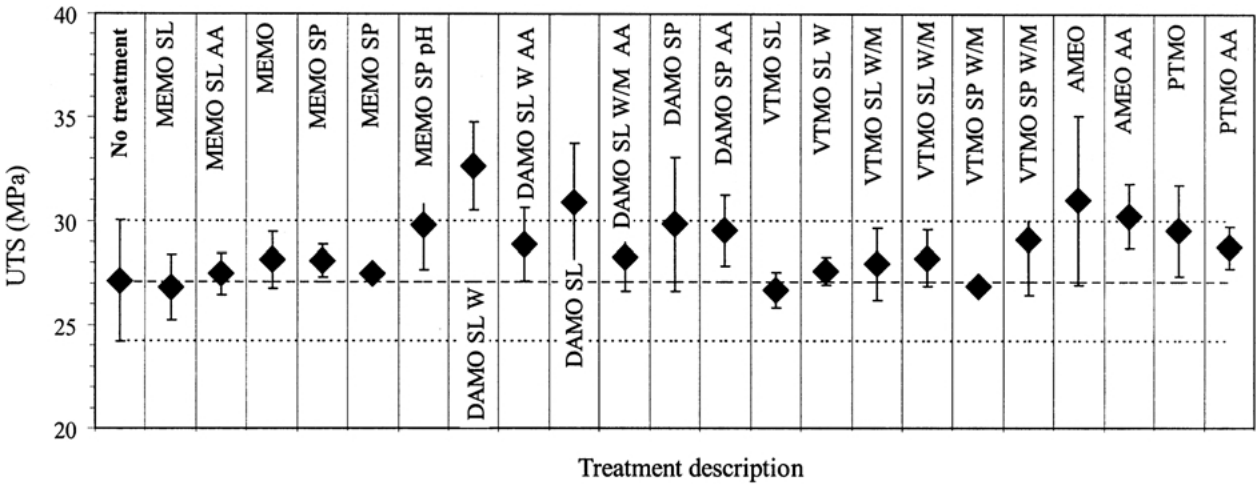

Figure 9 Ultimate tensile strength (UTS) for the HDPE/HAns composites (10% wt).

of the broader experimental window investigated (higher number of treatments applied) but also from the different HA characteristics, namely higher particle surface area, smaller particle size distribution and eventually higher surface chemical reactivity. Concerning HDPE/HAns composites, MEMO SP pH presents 27.5 MPa of UTS, while the MEMO SP pH AA presents 29.8 MPa of UTS (significantly different for a confidence level of 95%). The apparent effectiveness of the acrylic acid grafting on the tensile strength results from the interaction of the acrylic acid groups grafted into the HDPE chains with the organo-functional group of MEMO or with hydroxyl groups eventually available at the HA surface. Acrylic acid grafting of polyethylene was reported to be successful in increasing the interaction between polyethylene and hydroxyl groups at the surface of glass fibers [40]. The coupling methodologies based on amino silanes clearly differentiate from the remaining ones, originating the highest values of tensile strength. DAMO SL W, DAMO SL W/M and AMEO SL W and AMEO exhibit 32.6, 30.9 and 31.01 MPa of UTS, which accounts for increases of 20%, 14% and 14%, respectively as compared to standard HDPE/HA. Part of this success is associated to the simpler method for silane application, which makes the application of the coupling methodology based on amino silanes less dependent on factors such as pH and time of hydrolysis, since conversely to other cases, amine silanes readily dissolve in water, being the hydrolysis catalyzed by the alkalinity of the solution. Similar to the observed for the modulus, the acrylic acid grafting does not show any improvement in the tensile strength. The decreases in both the modulus and the strength upon grafting suggests that some, if not all, of the acrylic acid may be dispersed by the polymer matrix, with negative consequences at the mechanical performance level. A previous work on the chemical coupling of HDPE/HA composites [25] sustained the observed decrease in stiffness and strength upon acrylic acid grafting with a plasticizer effect of the acrylic acid on the polyethylene matrix.

Fig. 10 presents the variation of the ε_b for HDPE/HAns composites. All the coupling treatments maintain the high ductility of the HDPE/HAns composites ($\sim$ 450%). Mention should be made of the DAMO SL W formulation, for which the ductility is significantly improved to 650% together with the respective stiffness and strength previously mentioned.

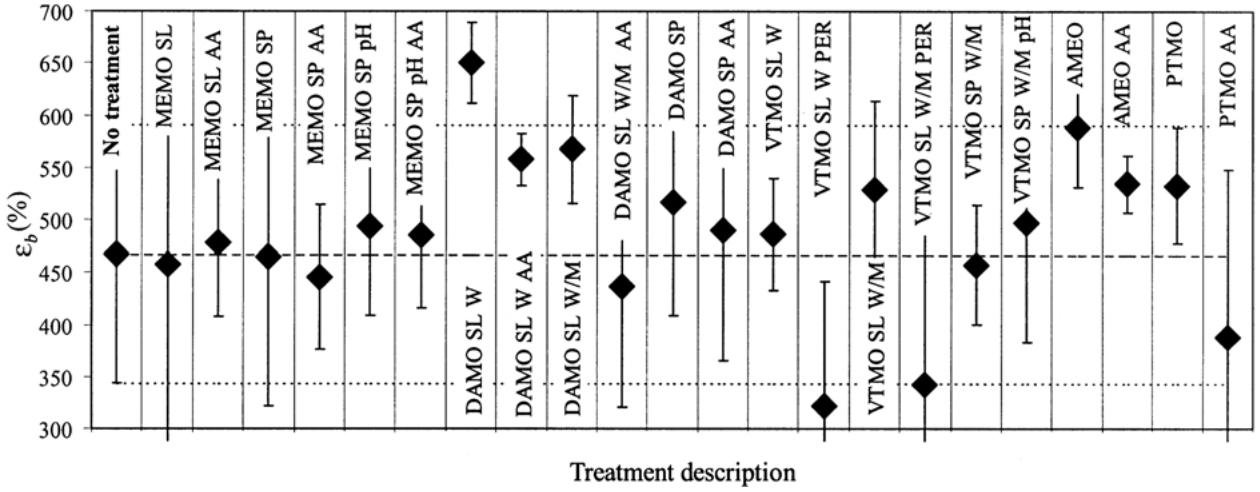

Figure 10 Strain at break (ε_b) for the HDPE/HAns composites (10% wt).

3.2. Morphology developed

3.2.1. HDPE/HAs composites

Fig. 11 presents the scanning electron microscopy (SEM) photographs of the tensile fracture surface of HDPE/HAs composites (Fig. 11(a)) and the typical HAs particle at the fracture surface (Fig. 11(b)), illustrating a poor interface with the HDPE matrix. After fracture, there is no evidence of adhesion between the HA particles and the HDPE matrix, where a gap between the two phases is clearly distinguishable. The interaction between the two phases is assured only by the mechanical interlocking developed upon the cooling of the polymeric phase.

In Fig. 12, the SEM photographs are presented for the tensile fracture surface of HDPE/HAs MEMO pH composites (Fig. 12(a)) and for the respective HA particle-polymer matrix interface (Fig. 12(b)). Conversely to that previously observed for the uncoupled composite, MEMO pH composites exhibit polymer fibrils attached the HA particles which appears to be an indication of improved adhesion between the phases. This observation of improved adhesion for this composite formulation is consistent with the respective mechanical performance improvement previously referred to. The apparent improvement in interfacial adhesion upon coupling is also evident for AMEO pH AA composites as observed in Fig. 13 that presents the SEM photographs of the fracture surface (Fig. 13(a)) and the interface between a HA and the HDPE matrix (Fig. 13(b)) for this composite. In this case, the wetting of the HA particles by the HDPE matrix is clearly improved upon the coupling treatment, making the interface between the two phases almost indistinguishable (Fig. 13(b)).

3.2.2. HDPE/HAns composites

Fig. 14 presents the SEM photographs of the typical fracture surface morphology (Fig. 14(a)) and the detailed view of an interface between a HAns particle and the HDPE matrix (Fig. 14(b)) for the HDPE/HAns composites. The HAns particle is contained within a deformed void generated during the mechanical loading of the matrix. The formation of voids and the occurrence of particle debonding is the combined result of both the ductile behavior of the matrix and the poor interfacial adhesion between the ceramic particles and the polymer.

The high ductility of DAMO SL W composites (ε_b of 650%) is evident by the extensive fibril formation at the fracture surface as it can be observed in Fig. 15. For the

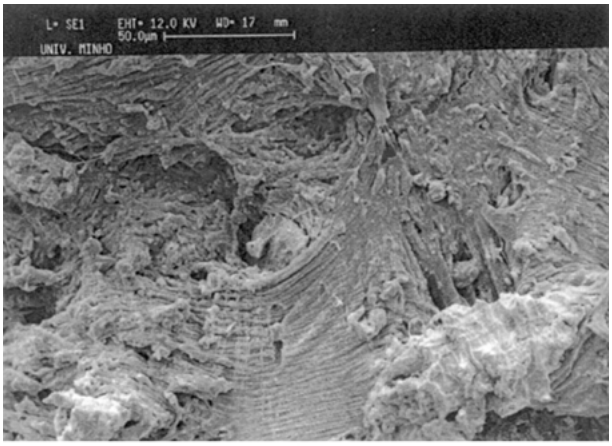

(a)

(b)

Figure 11 Scanning electron microscope (SEM) photographs of the fracture surface of HDPE/HAs composites showing (a) the respective morphology and (b) a typical HAs particle and respective interface.

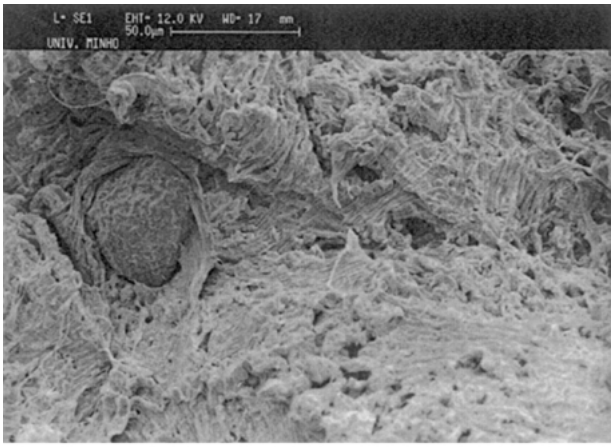

(a)

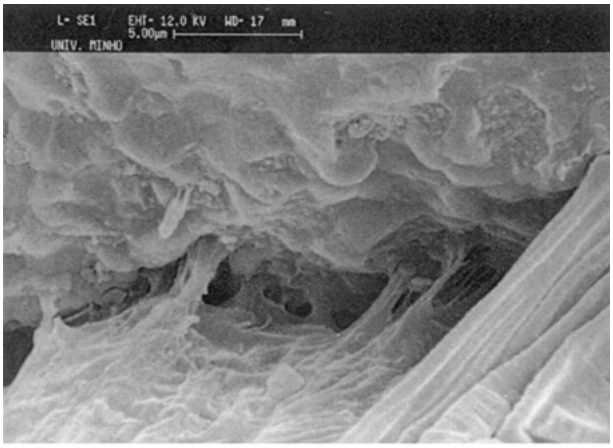

(b)

Figure 12 Scanning electron microscope (SEM) photographs of the fracture surface of tensile tested HDPE/HAs MEMO pH composites showing (a) the respective morphology and (b) the interface with between a HAs particle and the HDPE matrix.

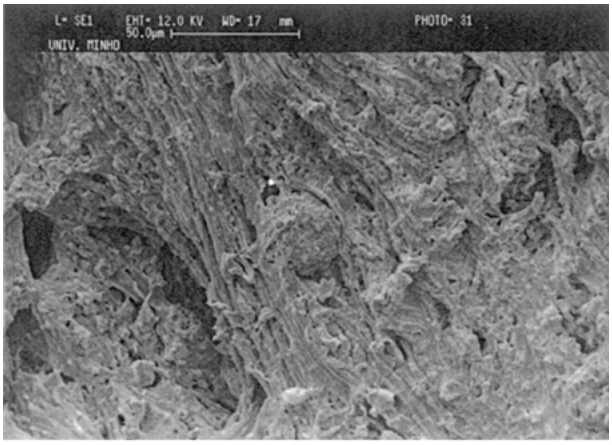

(a)

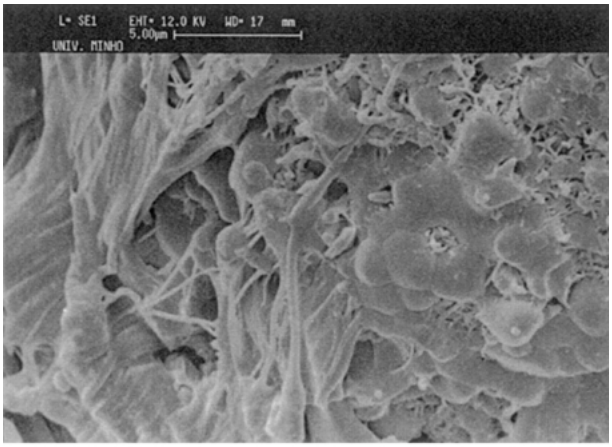

(b)

Figure 13 Scanning electron microscope (SEM) photographs of the fracture surface of tensile tested HDPE/HAs AMEO pH AA composites showing (a) the respective morphology and (b) the interface between a HAs particle and the HDPE matrix.

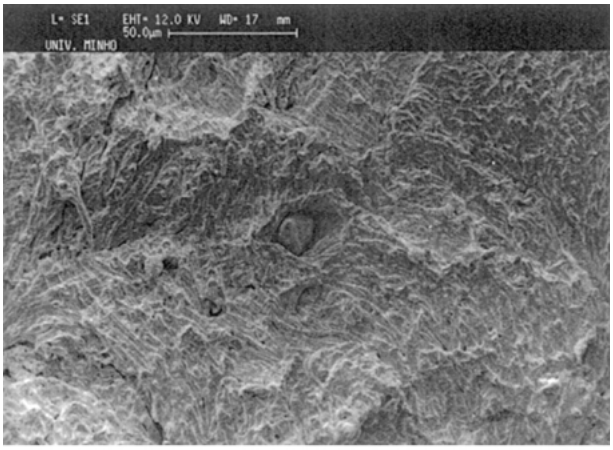

(a)

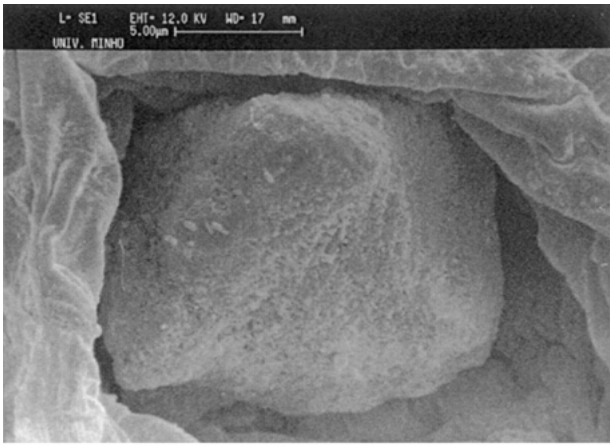

(b)

Figure 14 Scanning electron microscope (SEM) photographs of the fracture surface of tensile tested HDPE/HAns composites showing (a) the typical morphology and (b) a typical HAns particle and respective interface.

other coupled composites, the morphology of the fracture surface remained almost unchanged. Nevertheless, certain coupled methodologies introduced significant changes at the interface level. For these cases, void formation also occurred during plastic deformation, but, in most of the cases, the HA particles remained partially attached to the inner sides of the void, as an indication of improved adhesion. Fig. 16 presents the SEM photographs of the typical fracture surface (Fig. 16(a)) and of a HA particle (Fig. 16(b)) for VTMO SL W/M PER composites. In Fig. 16(a), the intense plastic deformation of the matrix upon loading is evident. In spite of this plastic deformation, the HA particle remains attached to the polymer matrix (Fig. 16(b)).

4. Conclusions

For the sintered HA (HAs) based composites, it was possible to enhance significantly the stiffness by means of coupling treatments. The treatments based on MEMO and AMEO are, on average, the most effective for enhancing the stiffness of HDPE/HAs composites, which is consistent with the improvement in interfacial adhesion observed by SEM. The low relative influence of these coupling procedures on strength is believed to be related to the low volume fraction and the relatively smooth surface of HA particles that limit the effect of the coupling procedures.

For the non sintered HA (HAns) composites, the coupling treatments based on MEMO and VTMO are the most effective concerning stiffness enhancement. Conversely to HAs composites, it was possible to significantly improve both the stiffness and the strength

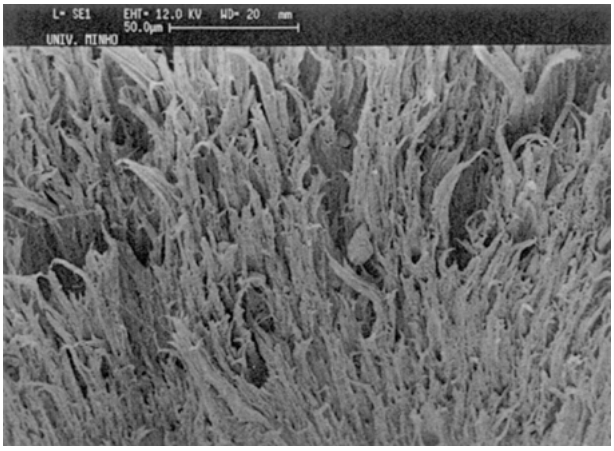

Figure 15 Scanning electron microscope (SEM) photograph of the typical fracture surface of HDPE/HAns DAMO SL W composites.

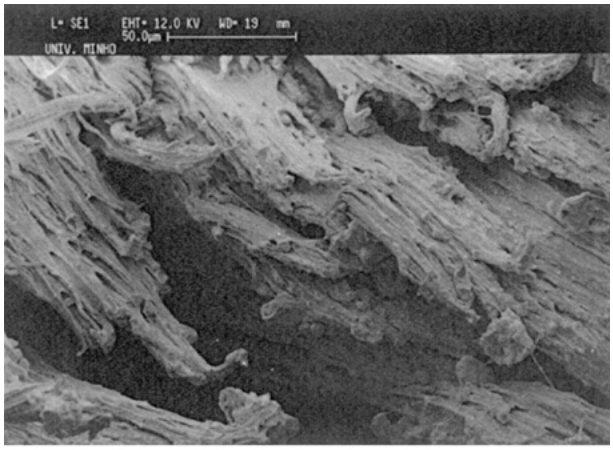

(a)

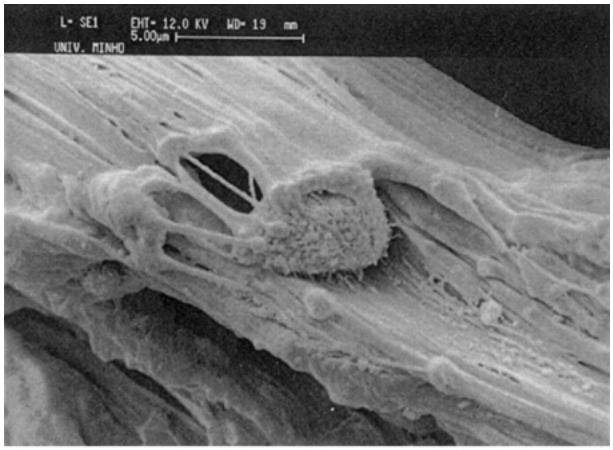

(b)

Figure 16 Scanning electron microscope (SEM) photographs of the fracture surface of tensile tested HDPE/HAns VTMO SL W/M PER composites showing (a) the respective morphology and (b) a HA particle partially encapsulated by the HDPE matrix.

for the HAns composites. Amino silanes were demonstrated to be highly efficient in relation to strength enhancement. The improvement in mechanical performance for the coupling procedures is consistent with the respective improvement in interfacial adhesion observed by SEM. The higher effectiveness of the coupling treatments for HAns composites is attributed to their higher particle surface area, smaller particle size distribution and higher chemical reactivity.

Several coupling treatment methodologies that can lead to significant mechanical performance improvement have been developed. The selection of the most promising coupling treatment and the respective optimization for higher HA volume fractions can lead to stronger bioactive composites that when appropriately processed may match the mechanical performance of human bone.

Acknowledgments

The author (RAS) acknowledges the financial support by Subprograma Ciência e Tecnologia do 2° Quadro Comunitário de Apoio, Ministério da Ciência e Tecnologia (Portugal).

References

1. W. BONFIELD, in ''Monitoring of Orthopaedic Implants'', edited by F. Burny and R. Pruers (Elsevier, Amsterdam, 1993), p. 4.
2. W. BONFIELD, *J. Biomech.*, **20** (1987) 1071.
3. T. S. KELLER, Z. MAO and D. M. SPENGLER, *J. Orthop. Res.*, **8** (1990) 592.
4. W. BONFIELD, M. D. GRYNPAS, A. E. TULLY, J. BOWMAN and J. ABRAM, *Biomaterials* **2** (1981) 185.
5. H. K. SCWYZER, J. CODEY, S. BRUM, P MATTER and S. M. PERREN, in ''Biomechanics'', edited by S. M. Perren and E. Schneider (1984).
6. A. J. TONINO, C. L. DAVIDSON, P. J. KLOPPER and L. A. LINCLAU, *J. Bone Joint Surg.* **58-B** (1976) 107.
7. M. WANG, N. H. LADIZESKY, K. E. TANNER, I. M. WARD and W. BONFIELD, *J. Mat. Sci.* **35** (2000) 1023.
8. N. H. LADIZESKY, I. M. WARD and W. BONFIELD, *J. Appl. Polym. Sci.* **65** (1997) 1865.
9. I. M. WARD, W. BONFIELD and N. H. LADIZESKY, *Polym. Int.* **43** (1997) 333.
10. J. HUANG, L. DI SILVIO, M. WANG, K. E. TANNER and W. BONFIELD, *J. Mater. Sci.: Mater. Med.* **8** (1997) 775.
11. J. HUANG, L. DI SILVIO, M. WANG, I. REHMAN, I. C. OHTSUKI and W. BONFIELD, *ibid.* **8** (1997) 808.
12. G. KALAY, R. A. SOUSA, R. L. REIS, A. M. CUNHA and M. J. BEVIS, *J. Appl. Polym. Sci.* **73** (1999), 2473–2477.
13. R. L. REIS, A. M. CUNHA, M. J. OLIVEIRA, A. R. CAMPOS and M. J. BEVIS, *Mat. Res. Innovat.* **4** (2001) 263–272.
14. R. A. SOUSA, R. L. REIS, A. M. CUNHA and M. J. BEVIS, *J. Appl. Polym. Sci.* **86** (2002) 2873.
15. R. A. SOUSA, R. L. REIS, A. M. CUNHA and M. J. BEVIS, *Plast. Rubb. Composites Proc. Appl.* Submitted.
16. R. A. SOUSA, A. L. OLIVEIRA, R. L. REIS, A. M. CUNHA and M. J. BEVIS, *J. Mat. Sci. Mat. Med.* In press.
17. J. DRELICH and J. D. MILLER, *Miner. Metallur. Process.* **12** (1995) 197.
18. J. Z. LIANG, R. K. Y. LI and S. C. TJONG, *Plast. Rubb. Compos. Process. Appl.* **26** (1997) 278.
19. L. TIEQI, G. LIU and K. QI, *J. App. Polym. Sci.* **67** (1998) 1227.
20. Z. A. MOHD ISHAK, A. AMINULLAH, H. ISMAIL and H. D. ROZMAN, *ibid.* **68** (1998) 2189.
21. S. H. PAK and C. CAZE, *J. App. Polym. Sci.* **65** (1997) 143.
22. C. H. TSELIOS, D. BIKIARIS, P. SAVIDIS, C. PANAYIOTOU and A. LARENA, *J. Mat. Sci.* **34** (1999) 385.
23. A. M. P. DUPRAZ, S. A. T. VAN DER MEER and K. DE GROOT, *J. Biomed. Mater. Res.* **30** (1996) 231.
24. K. NISHIZAWA, M. TORIYAMA, T. SUZUKI, Y. KAWAMOTO, Y. YOKUGAWA and F. NAGATA, *Chem. Soc. Japan* **5** (1990) 209.
25. S. DEB, W. WANG, K. E. TANNER and W. BONFIELD, *J. Mater. Sci.: Mater. Med.* **7** (1996) 191.
26. M. WANG, S. DEB and W. BONFIELD, *Mater. Lett.* **44** (2000) 119.
27. S. SHINZATO, T. NAKAMURA, T. KOKUBO and Y. KITAMURA, *J. Biomed. Mater. Res.* **55** (2001) 277.
28. A. M. P. DUPRAZ, S. A. T. VAN DER MEER, J. R. DE WIJN and J. H. GOEDEMOED, *J. Mater. Sci.: Mater. Med.* **7** (1996) 731.
29. Q. LIU, J. R. DE WIJN, K. DE GROOT and C. A. VAN BLITTERSWIJK, *Biomaterials*, **19** (1998) 1067.
30. Q. LIU, J. R. DE WIJN, K. DE GROOT and C. A. VAN BLITTERSWIJK, *J. Biomed. Mater. Res.* **40** (1998) 257.
31. R. A. SOUSA, PhD Thesis, Brunel University, 2002.
32. R. N. ROTHON, in ''Particulate-Filled Polymer Composites'', edited by R. N. Rothon (Longman Scientific & Technical, Harlow, 1995).
33. R. N. ROTHON and M. HANCOCK, in ''Particulate-Filled Polymer Composites'', edited by R. N. Rothon (Longman Scientific & Technical, Harlow, 1995).
34. B. PUKÁNSKY, in ''Particulate-filled Polypropylene:Structure and Properties, Vol 3, Composites'', edited by J. Karger-Kocsis (Chapman & Hall, Cambridge, 1995).
35. J. I. VELASCO, J. A. DE SAJA and A. B. MARTINEZ, *J. App. Polym. Sci.* **61** (1996) 125.
36. Q. WULIN, K. MAI and H. ZENG, *ibid.* **71** (1999) 1537.

37. A. K. SEN, B. MUKHERJEE, A. S. BHATTACHARYA, P. P. DE and A. K. BHOWMICK, *J. Therm. Anal.* **29** (1993) 887.
38. J. DE BOER, H.-J. VAN DEN BERG and A. J. PENNINGS, *Polymer* **25** (1984) 513.
39. A. G. ANDREOPOULOS and E. M. KAMPOURIS, *J. Appl. Polym. Sci.* **31** (1986) 1061.
40. I. KAMEL, M. J. KOCZAK and R. D. CORNELIUSSEN, *J. Appl. Polym. Sci. Polym Symp.* **23** (1974) 157.

Received 31 May
and accepted 19 August 2002